ECS Transactions, 16 (51) 23-31 (2009)
10.1149/1.3242219 ©The Electrochemical Society

# In Situ Synchrotron X-ray Spectroscopy of Lanthanum Manganite Solid Oxide Fuel Cell Electrodes

Kee-Chul Chang[a], Bilge Yildiz[b], Deborah Myers[c], John David Carter[c], and Hoydoo You[a]

[a] Materials Science Division, Argonne National Laboratory, Argonne, Illinois 60439, USA
[b] Department of Nuclear Science and Engineering, Massachusetts Institute of Technology, Cambridge, MA 02139 USA
[c] Chemical Sciences and Engineering Division, Argonne National Laboratory, Argonne, Illinois 60439, USA

We investigated the underlying physical and chemical causes of the improvement of electrochemical activity of the cathode in solid oxide fuel cells (SOFC) under long term cathodic or anodic polarization, termed 'current conditioning', through in situ X-ray absorption spectroscopy (XAS). The electrodes were powder $La_{0.8}Sr_{0.2}MnO_3$ (LSM) made with glycine-nitrate process and thin films of LSM and $La_{0.8}Ca_{0.2}MnO_3$ (LCM) grown by pulsed laser deposition (PLD), all on single crystal Yttria stablized Zirconia (YSZ) substrates. Changes in the XAS of the Mn K, La $L_3$ as well as the Sr K edge for LSM during current conditioning were studied. Our results shows no significant oxidation state changes for the Mn, but instead suggests that the redistribution of cation concentration profiles inside the pervoskite electrode may be the important factor in current conditioning.

## Introduction

The solid oxide fuel cell (SOFC) has potential to produce energy with high efficiency, especially when used for combined heat and power generation. SOFC using yttria-stabilized zirconia (YSZ) typically operate at temperature above 800°C, which negates the need for expensive Pt catalyst and permits fuel flexibility due to negligible CO poisoning effects. These properties make SOFC an ideal stationary mid-output power source.

Unfortunately, poor cathode performance is one of the major factors in preventing the widespread use of SOFC. To improve cathode performance, fundamental studies on the mechanism and kinetics of the oxygen reduction reaction are needed. Although varieties of ex situ methods can be used to investigate SOFC electrode before and after operation, there is always the lingering question of how to relate the analysis results to specific electrochemical mechanisms. In situ high temperature investigation of SOFC electrodes is needed in this regard and X-rays are an ideal probe for the high temperature and atmospheric pressure environment that are present under realistic SOFC operation.

In this paper, we focus on the changes that occur in the electrode of SOFC during initial application of potential, sometimes defined as 'current conditioning' in the literature. The electrode can improve (or sometimes worsen) in electrochemical activity after a period of initial polarization after which its performance stabilizes [1]. A better understanding of the cause of this phenomenon will lead to clearer insight on the factors

which affect SOFC electrode performance, resulting in the practical ability to design better electrodes.

There are various theories on the causes of current conditioning; Mn oxidation state change leading to an increase in the oxygen vacancies inside the perovskite [2], morphology changes in the electrode leading to a larger active surface area or interface [3,4], formation or removal of non-conductive secondary phases at the electrode-electrolyte interface [5], and removal of phases that block oxygen absorption from the surface [6]. All these theories were based on ex situ experiments. This paper focuses on the change of cation oxidation states and surface concentration during current conditioning using X-ray spectroscopy.

## Experimental

Sample Preparation

The initial samples for our experiment were porous $La_{0.8}Sr_{0.2}MnO_3$ (LSM), sintered on a single crystal YSZ(001) substrate (1x1cm area, 0.5mm thick) by the glycine-nitrate process as detailed in [7]. The resulting porous LSM is estimated to be about 20-30μm thick. Although the porous LSM sample better represents a typical SOFC cathode, the oxygen reduction reaction in such system will have multiple pathways, the effects of which will be averaged out and hard to isolate with our X-ray techniques. Subsequently, the rest of our samples were prepared by pulsed laser deposition (PLD) because the resulting dense films should limit the reaction pathway to only the bulk pathway and the smooth surface will enable depth sensitive X-ray measurements.

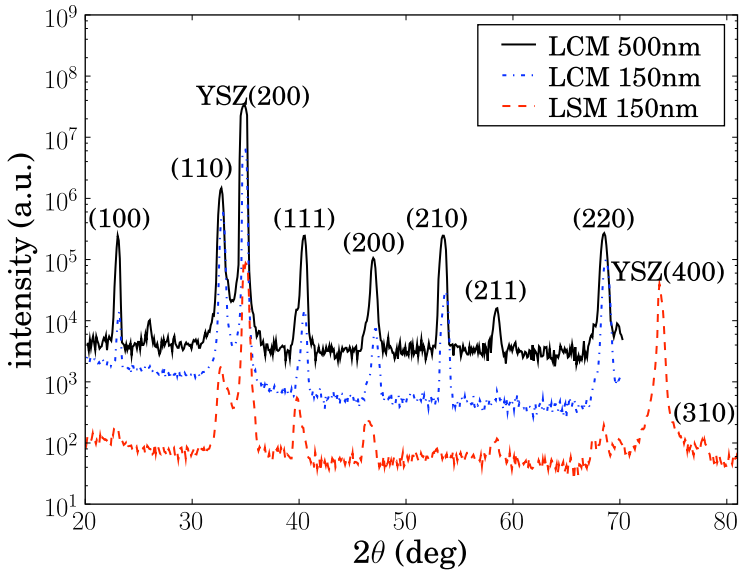


Figure 1. Cu Kα Rotating Anode X-ray theta-two theta scans on 500nm and 150nm thick LCM and 150nm thick LSM films.

Both LSM and $La_{0.8}Ca_{0.2}MnO_3$ (LCM) were grown on YSZ(001) substrates with the film thickness ranging from 10nm to 500nm with PLD. X-ray diffraction was taken on some of the films with a rotating anode to find whether the film has any epitaxial relation to the YSZ substrate and the results are shown in **Fig. 1**. The scans show that both the

LSM and LCM grow as a powder without a strongly preferred orientation with respect to the YSZ substrate. Only difference between the LCM and LSM films was that the (210) orientation growth seems to be preferred for the LCM while it is avoided on the LSM. Although some effort was put into varying the growth conditions of the perovskite films on YSZ(001), we were not able to grow completely epitaxial films with this substrate orientation.

In situ Electrochemical X-ray Cell

We prepared electrical contacts on the samples for in situ electrochemical measurements by fixing Pt mesh on the backside of the YSZ crystal and Pt wires on the perovskite surface with Pt paste as illustrated in **Fig. 2**. Since the powder LSM samples were relatively thick, we assumed that it would have sufficiently low in-plane resistance and used only the two thick side wires on the top surface. But the PLD samples had a middle wire, consisting of a thin Pt wire 50μm thick wire fixed in place with Pt ink. The incident X-rays were on this wire and parallel to it to insure that we were probing the area activated by the applied potential. The potentiostatic or galvanostatic measurements were done using a Princeton Applied Research 273A potentiostat.

Our experiments were preformed in the Materials Research Collaborative Access Team (MRCAT) insertion device beamline 10ID at the Advanced Photon Source (APS) at Argonne National Laboratory. The electrochemical cell was fixed on an alumina tube and the system was mounted on a 6 circle diffractometer. A photo of setup in operation is in **Fig 2**. We used an infrared spot heater (Research Inc.) to heat the sample to the desired temperature and a Vortex detector (Radiant Technologies) to measure the X-ray fluorescence from the sample for spectroscopy. In the current setup, we cannot control the oxygen pressure and the experiment was done in air.

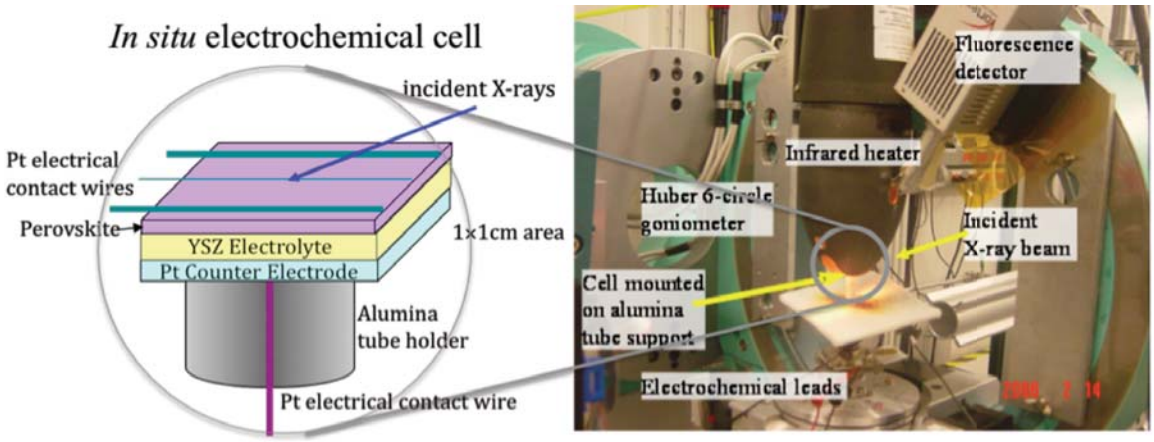


Figure 2. In situ electrochemical X-ray cell setup

A number of different X-ray characterization techniques could be used with this setup. In this paper, we focus the X-ray absorption near edge structure (XANES) of La, Sr and Mn to determine changes in the oxidation state of these cations coupled with grazing incidence X-rays for depth sensitivity. Since the index of refraction for X-rays in matter is less than 1, for an ideal flat surface there is total external reflection of X-rays below the critical angle;

$$\alpha_c \approx \lambda\sqrt{\frac{\rho r_0}{\pi}} \qquad (1)$$

where λ is the X-ray wavelength, ρ is the electron density of the material and $r_0$ is the classical electron radius. Below the critical angle, the X-ray weakly penetrate into the sample via an exponentially decaying evanescent wave. Therefore, by controlling the X-ray incidence angle, we can confine the penetration of the X-rays inside the perovskite film to its surface region as illustrated in **Fig 3**. Since the critical angle changes with the X-ray energy, its value will be noted with the X-ray energy.

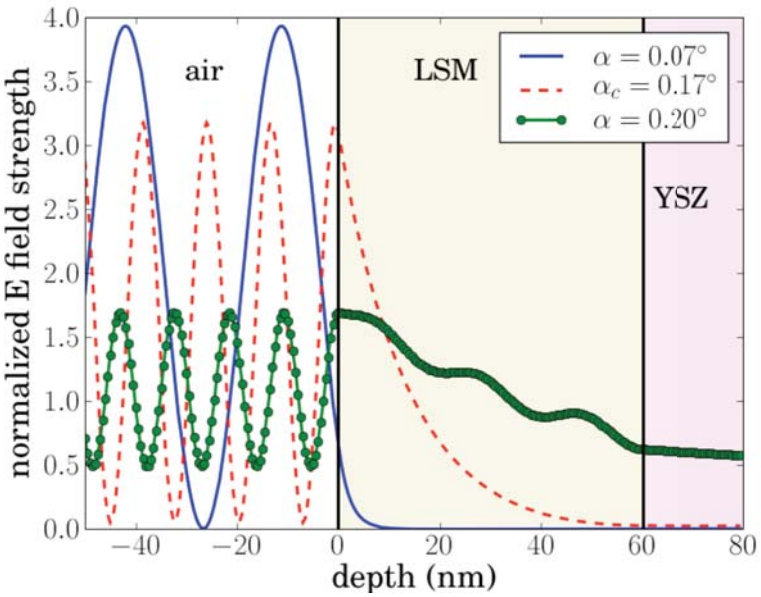


Figure 3. Illustration of the electric fields at different incidence angles for X-ray at 16.5 keV for a model LSM film on YSZ. The total fluorescence measured is roughly the integral of the concentration times the electric field strength, if absorption effects, which are minimal for thin films, are neglected.

The data presented in this paper focuses on experimental results that were found to be reproducible among the 24 samples, summarized in **Table I**, we studied.

**TABLE I.** Summary of the types samples and experimental measurements.

| **Type of sample** | **# of samples** | **Type of measurement done on # of samples** | | | |
|---|---|---|---|---|---|
| | | Mn K | La L2 | La L3 | Sr K |
| Powder LSM | 6 | 6 | 0 | 0 | 0 |
| PLD LCM | 8 | 5 | 5 | 2 | 0 |
| PLD LSM | 10 | 0 | 0 | 3 | 7 |

## Results and Discussion

X-ray Absorption Spectroscopy

We will first briefly go over what we can expect from X-ray spectroscopy. The cubic perovskite structure with a schematic diagram of its electronic band structure from molecular orbital theory [8] is shown in **Fig. 4**. There is large interaction between Mn

and the surrounding O ions in the octahedral cage, resulting in broad bands. The crystal field in the octahedral cage splits the Mn 3d bands into triplet $t_{2g}$ and doublet $e_g$ orbitals of different energy. The La and Sr has weaker interaction with its surrounding atoms, resulting in a narrower band.

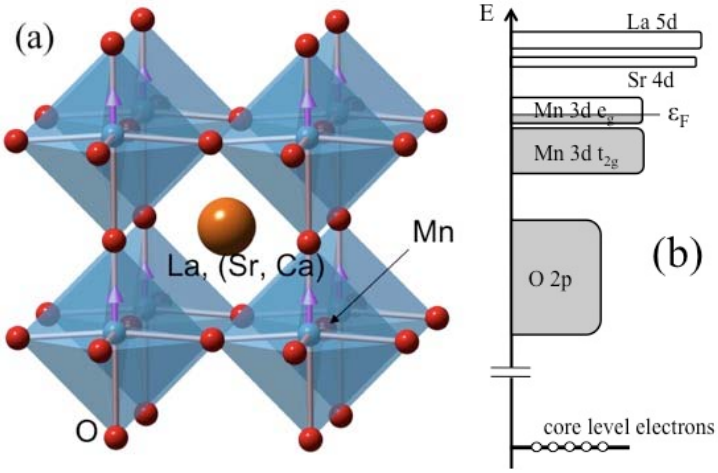


Figure 4. (a) Cubic perovskite structure (b) Schematic diagram of the band structure of LSM based on molecular orbital theory and theory calculations in reference [9]

In X-ray spectroscopy, we vary the X-ray photon energy across an edge threshold to induce transition of a core electron into an empty state. For synchrotron X-rays in an air environment, the edges that are easy to access are the Mn K, La L and the Sr K edges. The K edges, due to dipole selection rules, are most sensitive to electrons jumping from $1s_{1/2}$ to p states, which are far from the Fermi level. Weak quadropole transitions are also possible into the d states, especially when there is some intermixing of the d orbitals with the O p orbitals as in the case of Mn, resulting in a small pre-edge peak. The La $L_3$ edge detects transitions from the $2p_{3/2}$ into the d states.

Edge shifts occur for the K edge when the oxidation state changes due to slight binding energy shifts with the loss of electrons. This causes the edges to shift toward lower energy as the oxidation state increases.

So we can conclude that we will be most sensitive to the Mn and Sr oxidation states in our XANES results. If we are looking for changes in the electronic structure around the Fermi level, it should show the most prominently at the Mn pre-edge peak.

Mn K edge results

We first focused on the Mn K edge because we expected that any oxygen vacancy change would be reflected in a change in the Mn oxidation state. In porous LSM, we saw significant Mn K edge shifts upon heating as shown **Fig. 5a**. When cathodic potential was applied to the sample at high temperature, we found no evidence of edge shift with current conditioning as shown in **Fig. 5b**. This result was later reproduced in PLD LCM. As it can be seen in the figure, the only changes we observed with current conditioning were slight changes in the normalized peak intensity of the Mn XANES but this did not appear to be significant.

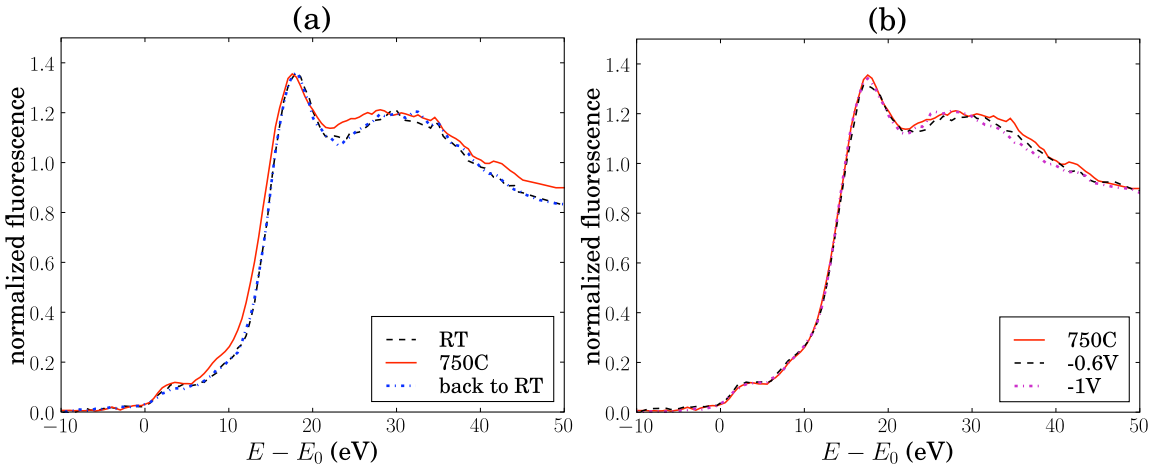


Figure 5. Porous LSM results showing that (a) Mn K edge shifts with temperature but (b) Mn XANES does not change with applied potential at 750°C

Note that although we see no evidence of Mn oxidation state change, it cannot be totally ruled out because we are averaging over a large area of the sample. Mn oxidation changes around a small area near the contact wires or at the electrode-electrolyte interface will be hard to determine with our techniques. Nevertheless, we can safely conclude that there is no large scale oxidation state change of the Mn at applied potential.

La L edge results

The La $L_3$ XANES has a large peak above the edge, often called the 'white line', due to electron transitions into the empty La d band states. Since the d band electrons empty out as the oxidation state become higher, the white line increases. For the flat PLD films, we observe that the intensity of this white line becomes greater as the measurements become more surface sensitive at lower incident angle, which is shown in **Fig. 6**. This suggests that the electronic structure around the La on the surface is different from that of the bulk. The increased white line could be an effect of surface termination and defects resulting in the surface La having more vacant d bands around it.

Also the unnormalized La fluorescence far above the La $L_3$ edge can be used as a rough measure of the La concentration. We compare the surface sensitive white line intensity and La concentration with applied potential in **Fig. 7** at a fixed incidence angle below the critical angle. These variations could not be seen for both cases at incidence angles above the critical angle, suggesting that the cause of this variation is due to changes near the surface.

The white line intensity (**Fig. 7a**) stayed almost constant when cathodic potential was applied but dropped off noticeably at anodic potential. But the surface La concentration (**Fig. 7b**) decreased at cathodic potential and decreased at anodic potential. This suggests that the potential is inducing the La cations in the film to move towards or away from the surface. The white line shows that for the cathodic case, surface concentration changes does not cause a change in the unfilled d bands state, while for the anodic case the d band states is partially filled, possibly by a change in the La oxidation state.

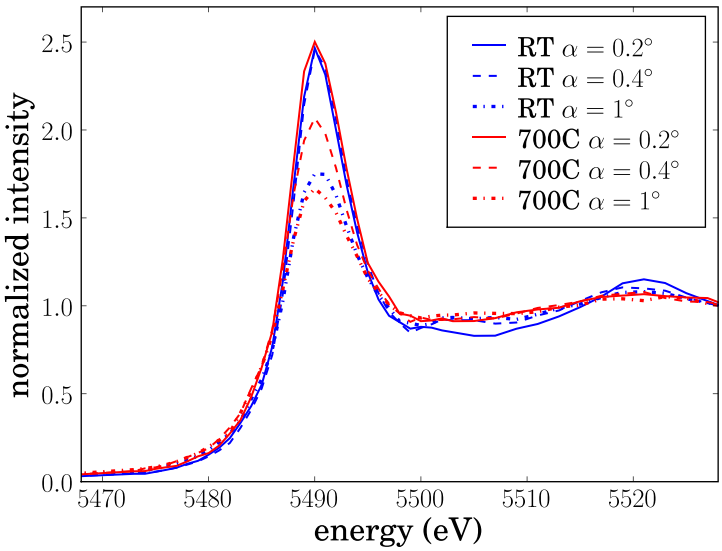


Figure 6. La $L_3$ XANES white line variation with temperature and X-ray incidence angle on 100nm thick PLD LSM. The critical angle $\alpha_c = 0.5°$ at 5.6keV.

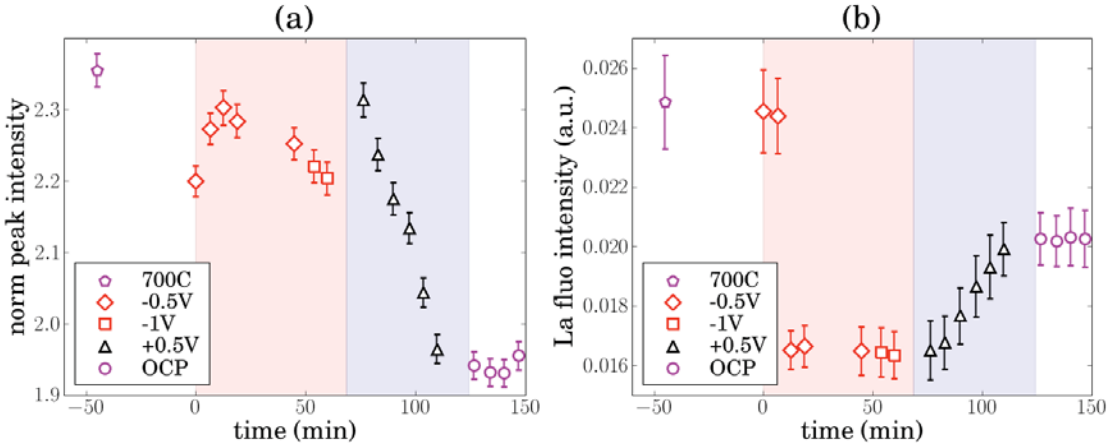


Figure 7. 150nm thick LSM results at 700C (a) La $L_3$ XANES white line and resistance changes (thick lines) with applied potential for incident angle $\alpha = 0.2°$ (b) La fluorescence changes with applied potential below the critical angle ($\alpha = 0.2°$, small markers) and above the critical angle ($\alpha = 1°$, large filled markers). Note that high angle markers are plotted on a different scale marked on the right.

Sr fluorescence results

We have also looked at the Sr K edge XANES in PLD LSM and found no measurable edge shifts with temperature and with applied potential. The only major changes that we found were changes in the Sr fluorescence intensity, which is shown in **Fig. 8**. Note that there is an increase in Sr at the surface at anodic potential, similar to what we found in the case for La. But in the Sr case, the increase in fluorescence intensity is much higher. This may be due to the fact that Sr occupies only 20% of the A sites in the perovskite

lattice, causing a large increase in the relative fluorescence intensity when it segregates to the surface.

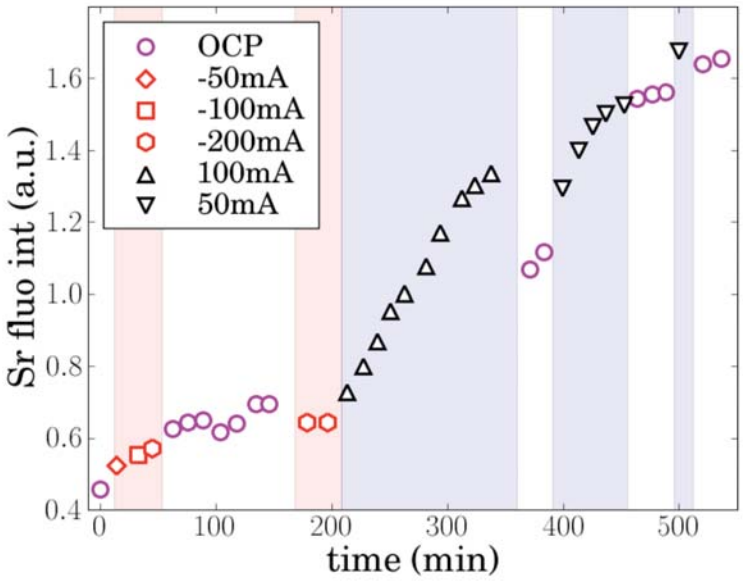


Figure 8. Sr fluorescence and resistance changes with applied potential for 150nm thick PLD LSM. $\alpha = 0.1°$, $\alpha_c = 0.17°$ at this energy of 16.3keV.

## Conclusions

The underlying causes for current conditioning were examined by the use of in situ X-ray spectroscopy. We find no evidence of Mn oxidation state changes with applied potential but there are white line changes in the La $L_3$ edge which suggests that the surface La oxidation state decreases at anodic potentials. We also find evidence of La and Sr segregation to the surface at anodic potentials.

These results show that the Mn oxidation state change is not a major factor in current conditioning. Kinetic demixing effect induced by the applied potential on the La and Sr cations is likely to be a bigger a factor, at least in the anodic case. There is fairly recent body of literature which suggests that Sr is thermodynamically driven to segregate to the surface [10, 11] but our results suggest that it can also be induced to segregate by potential.

## Acknowledgments

We acknowledge Dr. Beihai Ma for preparing the PLD LSM and LCM electrodes for this study and Dr. Bruce Ravel for the beamtime support at MRCAT. MRCAT operations are supported by the Department of Energy (DOE) and the MRCAT member institutions. This research was funded by the Laboratory Directed Research and Development Program at US-DOE's Argonne National Laboratory.

## References


1. S. B. Adler, *Chem. Rev.*, **104**, 4791 (2004).
2. H. Y. Lee, W. S. Cho, S. M. Oh, H. D. Wiemhofer, and W. Gopel, *J. Electrochem. Soc.*, **142**, 2659 (1995).
3. M. Kuznecov, P. Otschik, P. Obenaus, K. Eichler, and W. Schaffrath, *Solid State Ionics* **157**, 371 (2003).
4. S. P. Jiang, and W. Wang, *Solid State Ionics,* **176**, 1185 (2005).
5. A. Mitterdorfer, and L. J. Gauckler, *Solid State Ionics,* **111**, 185 (1998).
6. S. P. Jiang, and J. G. Love, *Solid State Ionics*, **138**, 183 (2001).
7. L. A. Chick, L. R. Pederson, G. D. Maupin, J. L. Bates, L. E. Thomas, and G. J. Exarhos, *Matter. Lett.*, **10**, 6 (1990).
8. R. Hoffman, *Angew. Chem. Int. Ed. Engl.,* **26**, 846 (1987).
9. H. Modrow, S. Bucher, J.J. Rehr, and A.L. Ankudinov, *Phys. Rev. B*, **67**, 035123 (2003).
10. H. Dulli, P. A. Dowben, S. H. Liou, and E. W. Plummer, *Phys. Rev. B*, **62**, R14629 (2000).
11. N. Caillol, M. Pijolat, and E. Siebert, *Appl. Surf. Sci.,* **253**, 4641 (2007).